Investigation of the effect of a plastic ring on the uniformity of ice layers in cryogenic inertial confinement fusion targets

Frank Fan

Webster Schroeder High School
Webster, NY

Advisor: Dr. R. S. Craxton
Senior Scientist

Laboratory for Laser Energetics
University of Rochester
Rochester, NY

Abstract:

A program has been written to model the evolution of the cryogenic ice layer during the layering of a target for inertial confinement fusion. The program simulates the thermal diffusion in the layering sphere, as well as the sublimation and deposition of the deuterium. This will facilitate the design and production of more-uniform targets. It has been found that any nonuniformities caused by the plastic rings of the recently proposed "Saturn" targets are too small to significantly impact fusion performance.

1. Introduction

Controlled nuclear fusion is a promising technology for producing clean, abundant energy. Laser-based inertial confinement fusion (ICF) is one method under investigation for producing the extreme temperatures and pressures required for fusion reactions to occur. In direct-drive ICF, an array of powerful laser beams fires upon a target from many directions, heating and compressing the target[1]. The target is a spherical plastic shell containing the hydrogen isotopes deuterium (D_2) and tritium (T_2). When the target is compressed, the deuterium and tritium nuclei fuse to form helium nuclei and energetic neutrons. (Another approach, indirect-drive ICF[2], involves laser beams entering the target chamber from the top and bottom and irradiating an x-ray-producing target. These x-rays then "indirectly" drive the spherical fuel-containing target.) Targets used in current laser-based ICF experiments generally contain only deuterium, as tritium is radioactive and hard to work with.

Cryogenic targets are spherical plastic shells with thin layers of solid deuterium and tritium on the inner surface of the shell. By using solid fuel, cryogenic targets can store much more fuel than traditional, gas-filled targets, increasing the likelihood of a

chain reaction. The plastic shells are first filled with gaseous deuterium and tritium, which are transformed to solid when the shells are cooled down. The target is then slowly heated in a device called a layering sphere to generate a more even ice layer, which improves the fusion performance.

Unfortunately, the heating inside the layering sphere is not perfectly uniform. For example, the so-called "Saturn" targets[3] for polar direct drive at the National Ignition Facility have small plastic rings around the equators, which can cause uneven heat conduction in the layering sphere. This can introduce nonuniformities in the ice layer, reducing the fusion performance. As the "Saturn" target has only been proposed very recently, it is not clear how severe the ice nonuniformity would be and whether it would have a significant impact on fusion performance. A program has been written to model the evolution of the cryogenic ice layer during the layering process, including simulation of the thermal diffusion in the layering sphere as well as the sublimation and deposition of the deuterium. The program was initially intended to answer the "Saturn" ring target question, but it is also flexible enough to model other target designs. It is believed to be the first program of its type.

1.1 Cryogenic targets

Cryogenic targets currently being used on the OMEGA laser system[4] are about 900 μm in diameter and contain solid deuterium. A cryogenic target typically has a 3 μm-thick plastic shell, with a 100 μm-thick deuterium ice shell on the inner surface of the plastic shell. The center contains deuterium vapor (see figure 1).

1.2. Cryogenic target formation

The formation of the cryogenic target involves several steps. First, a spherical
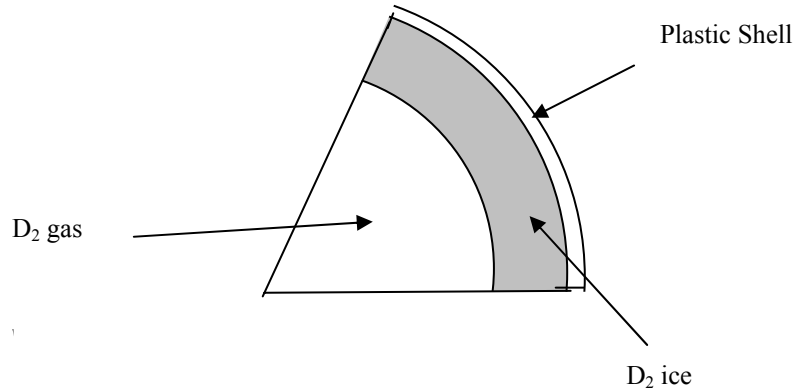
Figure 1: Cryogenic target cross section

plastic shell is filled, through diffusion, with deuterium gas to a pressure of about 1000

atm. The target is then cooled below the triple point of D_2, first entering the liquid phase,

then freezing into a layer of solid D_2. The D_2 layer is not uniform, as gravity pulls the D_2

to the bottom of the shell when it is in the liquid phase. Then, the target is

placed in a layering sphere (figure 2), a spherical cavity with reflective, gold-coated

walls[5]. An optical fiber is used to introduce low-power infrared light into the layering

sphere. The light reflects off the walls and is absorbed by the D_2 ice. The rough surface of

the wall ensures that the infrared light is scattered in all directions. In addition, the

infrared light may bounce back and forth several times before it hits the target.

Consequently, the target is heated uniformly in all directions. The thicker areas of the ice

absorb more light and become hotter than the thinner areas. The ice in the thicker areas

sublimes faster than the ice in the thinner, cooler areas, and the resulting gas
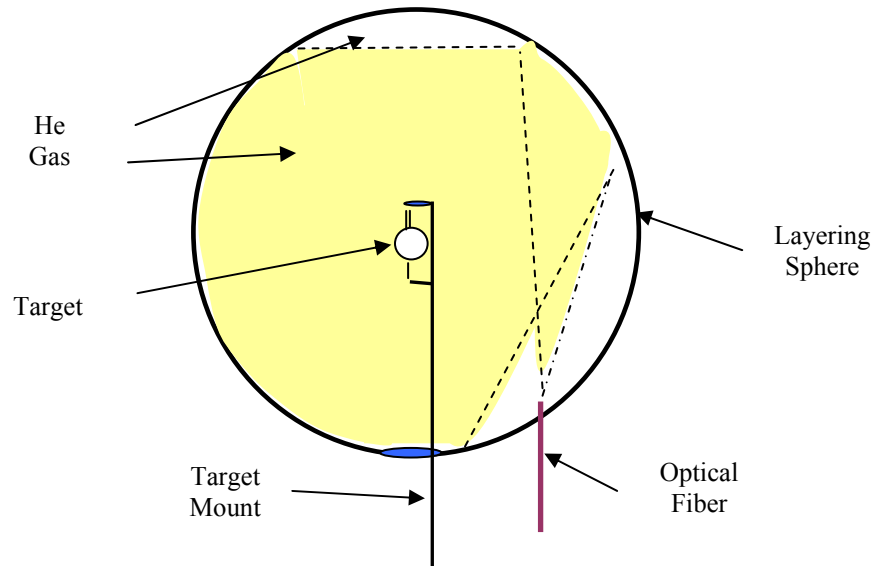
Figure 2: Layering sphere. The target is supported by a target mount. The
optical fiber introduces the infrared light (yellow area), which is scattered
from the wall and heats the target uniformly. The helium gas in the
layering sphere conducts the heat from the target to the wall.

preferentially condenses on the cooler, thinner areas (figure 3). The heat is removed from

the target by conduction through the helium gas to the wall of the layering sphere, which

is kept at a constant temperature of 18.6 K. The layering process takes about 24 hours,
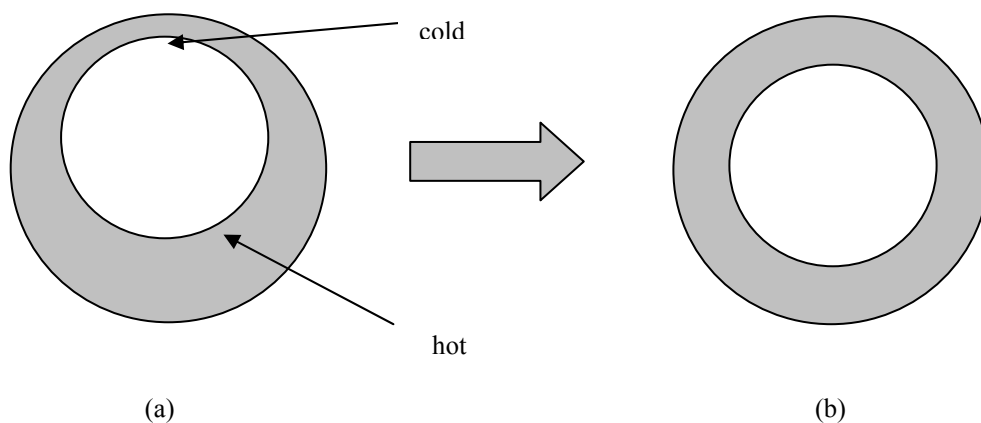

(a) (b)

Figure 3: A cryogenic target (a) before and (b) after the layering process. The thicker portions
become hotter due to heating by infrared light, so deuterium sublimes from the thick portions and
deposits on the thin portions, resulting in a more even ice layer.

and results in an isotherm along the inner surface of the ice layer. An even ice layer is required because an uneven ice layer results in uneven compression and poor fusion performance. A nonuniformity of 1% can be tolerated in the ice layer. In a 100 μm ice layer, this translates to a nonuniformity of 1 μm.

1.3 Saturn Targets

The National Ignition Facility (NIF) is a facility for laser-based ICF research scheduled for completion in 2010. The new, 192-beam laser is designed to deposit 1.8 MJ of energy on a target 3 mm in diameter. The greater amount of fuel in the larger targets increases the probability of an energy gain, in which the fusion energy generated is greater than the input laser energy. However, the NIF is designed to perform indirect-drive laser-based ICF experiments and has no laser beams aimed at the equator of the target. To perform direct-drive experiments, a novel target design has been proposed.
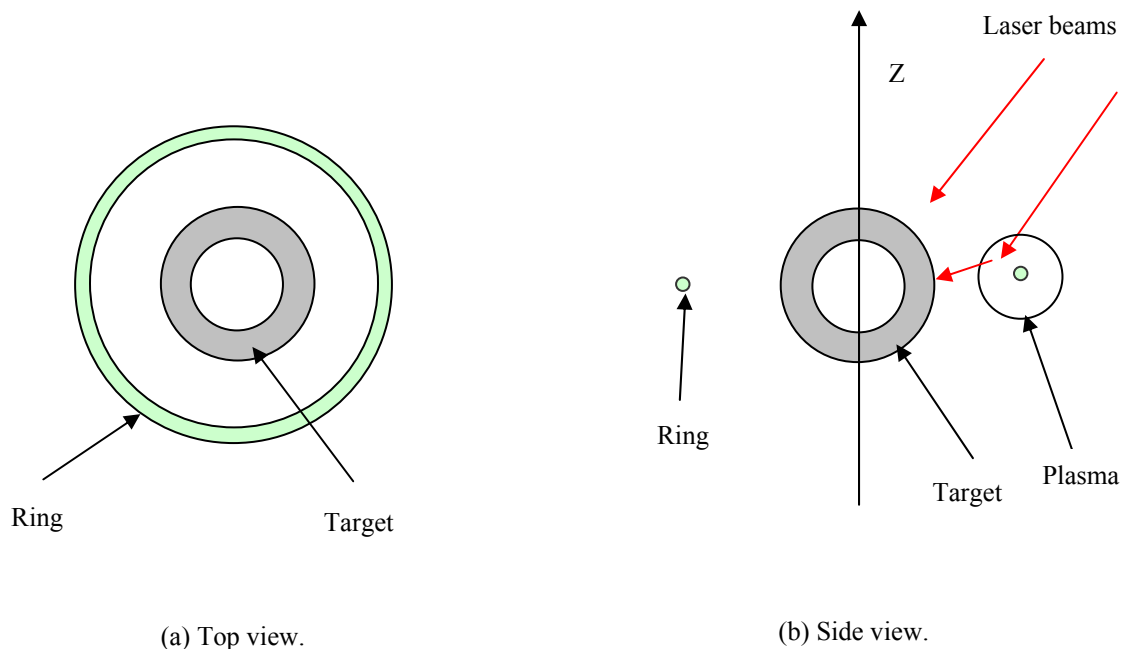

(a) Top view.

(b) Side view.

Figure 4: "Saturn" target.

The new target, the so-called "Saturn target," has a small plastic ring around the equator (figure 4)[3]. When the laser is fired, the plastic ring forms a plasma, which causes some of the laser beams to refract, striking the target at the equator.

The Saturn target raises uncertainty in layering. The ring has a higher thermal conductivity than the helium gas in the layering sphere. Hence, more heat is conducted from the equatorial regions of the target than from the polar regions. This causes the ice in the equatorial regions to be thicker than that in the polar regions. However, the degree to which the ring affects the ice thickness is not known.

The primary goal of this project is to ascertain the effect of the ring on the ice layer and, in particular, to determine the size of the ice perturbation.

2. The Program

The project entailed writing a program to model the formation of the ice layer in a cryogenic target. The user defines the target structure, an initial ice layer (specifically the radius of the inner ice surface for each direction (θ, φ) with respect to the vertical axis), and an initial temperature for each part of the system. The infrared heating of the target and the sublimation and condensation of the ice layer are simulated over a period of time defined by the user. The program displays the result with plots showing the new location of the ice layer, as well as the temperature contours inside the target.

The entire layering sphere, including the cryogenic target, is divided into three-dimensional (3-D) grid cells, of which 2-D cross sections are shown in figure 5. This is done in spherical geometry, along the r, θ, and φ dimensions. The grid is typically chosen to be denser in the ice layer, especially near the interface between the ice and gas.

(The fine zoning is expanded beyond the ice layer to accommodate simulations involving severe ice nonuniformities.)
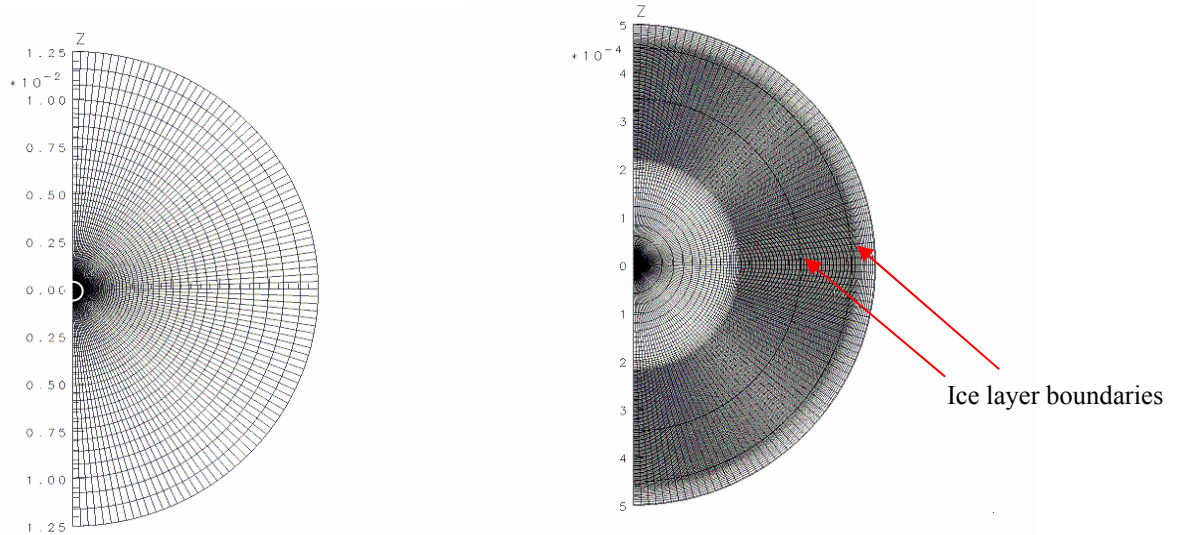

Figure 5: (a) The entire layering sphere divided into grid cells (outer radius=1.25 cm), and (b) the area outlined in white in greater detail (radius = 500 μm). Note the high density of grid cells in and near the ice layer, whose boundaries are shown with dark lines.

The temperature of each cell is stored in a 3-D array, as are the thermal conductivity, the specific heat, and the amount of heat each cell receives from the infrared laser. A two-dimensional array, indexed in the θ and φ directions, keeps track of the radius of the ice-gas interface. Although this particular problem (Saturn ring) is 2-D in nature due to the symmetry in φ, the program was written in 3-D to allow for more complex future applications. The program performs a large number of time steps, each of which is typically a small fraction of a second. During each time step, the new temperature of each cell is calculated, taking into account the infrared heating and thermal conduction. The amount of sublimation and condensation at each interface cell is also calculated, and the new radius of the interface is determined.

The rate of sublimation is a function of the temperature of the solid. Although it is not a linear function, we are working with a very small temperature range near equilibrium. Thus, $\frac{dN_s}{dt}$, the rate of sublimation per unit area in molecules/m^{2}s, is linearized as:

$$\frac{dN_s}{dt} = N_0 + \alpha(T_{solid} - T_{ref}),$$ (1)

where T_{ref} is the reference temperature of 18.6 K, T_{solid} is the temperature of the deuterium ice, N_0 is the rate of sublimation at the reference temperature, and α is a constant coefficient. (See the appendix for numerical values of α and other physical constants.)

Similarly, $\frac{dN_c}{dt}$, the rate of deposition is linearized as:

$$\frac{dN_c}{dt} = n_{gas}\left[\beta - \gamma(T_{gas} - T_{ref})\right],$$ (2)

where T_{gas} is the temperature of the gas, n_{gas} is the density of the gas in molecules per cubic meter, and β and γ are constant coefficients. Subtracting (1) from (2) gives the overall rate of deposition of molecules per unit area:

$$\frac{dN}{dt} = n_{gas}[\beta - \gamma(T_{gas} - T_{ref})] - N_0 - \alpha(T_{solid} - T_{ref}),$$ (3)

In addition, the thermodynamic activity is modeled by the following:

$$\frac{\partial}{\partial t} C_v T = \nabla \bullet \kappa \nabla T + Q_{IR} + Q_L,$$ (4)

where C_v is the specific heat, T is the temperature, κ is the conductivity, Q_{IR} is the infrared heat, and Q_L is the latent heat per unit volume, which is proportional to the rate of deposition of molecules per unit area. It seems reasonable to deposit the latent heat in

the solid (rather than the gas) as the slow molecules in the thermal distribution in the gas

will excite lattice vibrations in the solid lattice when they are captured. Some of this

energy may return to the gas through thermal conduction.

The latent heat is believed to be deposited over a very thin layer, but its

distribution is difficult to determine. However, since the thermal conduction will rapidly

remove the steep gradients, the exact distribution is not very important here. Numerically,

we deposit all the latent heat in the first boundary cell that contains ice. This cell will

have

$$Q_L = \frac{L}{\Delta x} \frac{dN}{dt} \;, \tag{5}$$

where L is the latent heat per molecule and Δx is the ice thickness in the cell.

The sublimation and heat transfer occur simultaneously. To calculate the

temperature changes, the amount of sublimation that occurred and thus Q_L must be

known. Also, the temperatures of the ice and gas at the interface must be known to

determine the amount of sublimation that occurs. However, to solve the sublimation and

heat transfer in one step would be difficult and computationally intensive, so it was

decided to decompose them into two separate procedures. We have separated the problem

into a linear equation (Equation (4)) and a few linear and nonlinear function evaluations

(Equations (3) and (5)). The heat transfer equation has been well studied. Many mature

algorithms exist that can efficiently solve this equation. Equations (3) and (5) can be

evaluated in a straightforward manner. As the time step is small the error introduced due

to the separation of heat transfer and sublimation/condensation is negligible.

The ice radii calculated after each time step typically do not fall on a cell border.

As a result, the interface cell contains both ice and gas (see figure 6). The cells across the

ice-gas interface are modeled using a linear mixture of parameters from both ice and gas,
according to the ice/gas ratio within the cell. Specifically, once the ice radii are evaluated,
the cells are searched to determine which ones contain the interface. The gas and ice
volumes within the interface cells are calculated. The specific heat and the conductivity
of the cell are then computed as

$$C_v = pC_{vGas} + (1-p)C_{vSolid} \ , \tag{6}$$

and

$$\kappa = p\kappa_{Gas} + (1-p)\kappa_{Solid} \ , \tag{7}$$

where p and *(1-p)* are the proportions (in volume) of gas and solid contained in the cell,
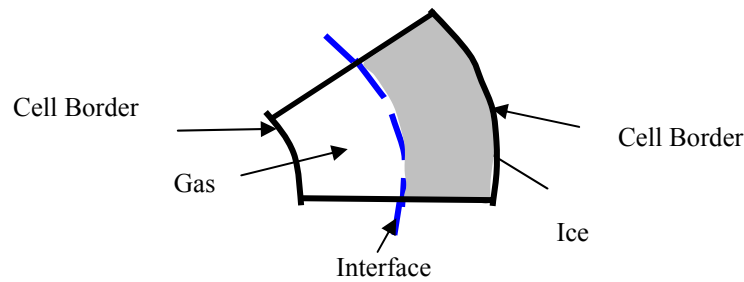respectively.

Figure 6: Cell containing the gas/ice interface. Both ice and gas are
present in the cell.

A natural approach to predicting the ice shape at the end of the layering process is
to set the initial condition to be as representative of the real situation as possible, and run
the simulation for the same duration as the real process. As the software time step is
typically a few hundred microseconds and the layering requires 24 hours, the number of
time steps required is in the hundreds of millions. Two issues emerged with this huge
number. First, it would take days to perform one simulation, even with a modern
computer. Second, computation errors, such as rounding errors, accumulate during each

step of the calculation. The total error, which is proportional to the number of steps, may be large enough to make the calculation meaningless. The introduction of variable time step techniques, which will be discussed later, can reduce the number of time steps by a factor of about five. However, the resulting number of steps is still extremely large.

It was decided to try a different method. When the layering process approaches the end, the system typically enters a steady state, which means that each part of the system remains almost unchanged. In our application, steady state implies that the sublimation is balanced by condensation, and the temperature of each cell remains constant. The steady state is determined by the system configuration including boundary conditions, heat sources, etc. It is very insensitive to a wide range of initial conditions. Consequently, we may calculate the steady state solution with a small amount of steps if we can find an initial condition (including initial ice geometry and initial temperature) that is close to the steady state. It turns out that this is not a very difficult task. It is known that the steady state for the target without the Saturn ring is a uniform shell. The introduction of the ring does change the steady state. Nevertheless, the magnitude of the change is relatively small. As a result, it can be reasonably assumed that using a uniform shell as the starting point, the simulation may reach the steady state in a short period of time.

Another method of reducing the number of time steps involves applying variable time steps. Specifically, during the initial transition period when the system drastically changes, a smaller time step is applied. Afterwards, when the system is near the equilibrium temperature, we take relatively large time steps. This variable step size scheme was developed based on several observations. A large step size saves time steps,

but it may cause significant calculation error and even instability. The step-by-step

calculation of equations (3)-(5) assumes that within each time step the system variables

including ice radius and cell temperature do not change very much and thus can be

approximated as constants and linear functions. The above assumption could be violated

once a large time step is adopted. However, we noticed that the error in approximation

does not only depend on the time step size, but also on how quickly the system changes.

When the system remains steady, even a relatively large step does not introduce

noticeable error. As a result, the variable time step size approach serves both our goals:

fewer time steps and acceptable calculation error. The maximum ice thickness increment

is used as an indicator for the system change. The time step size is determined to be

inversely proportional to the indicator. A ceiling is imposed to prevent too large a step

size when the change on the previous step approaches zero. More specifically, the step

size for step i is determined as

$$\Delta t(i) = Min(\frac{\Delta r_d \Delta t(i-1)}{Max_{\theta\varphi} \mid \Delta r_{\theta\varphi}(i-1) \mid}, \Delta t_{max}) , \qquad (8)$$

where Δt_{max} is the maximum step size allowed, Δr_d is the desired radius change, typically

around 10 pm. $\Delta r_{\theta\varphi}$ (i-1) is the ice radius change in the direction of (θ, φ) that occurred in

the previous time step, Δt (i-1) is the size of the previous time step, and the maximization

is over all directions. This variable step size approach results in a reduction of the number

of the steps by a factor of about five.

3. Results

The ice shape of the layered "Saturn" target was determined using the program.

As discussed in Section 2, the initial condition was set with an ice layer of uniform

thickness. The heat absorption of the ice was set at about 46 kW/m^3, approximately the same as the heat produced through beta decay of deuterium-tritium ice[6,7]. The target has a diameter of 900 μm, an ice layer thickness of 100 μm, a ring cross section diameter of 300 μm, and a ring major radius (distance from the center of the ring to the origin) of 1100 μm. The results are summarized in Figures 7 through 9.

Figure 7 shows temperature contours for the target, (a) at time $t = 5$ seconds and (b) after an hour, plotted in polar coordinates. The lines in the contour maps are isotherms, representing locations with the same temperatures. The ice surface radii, which are not plotted, are about 347 μm in both figures (the deviations of the actual radii are too small in scale to be seen in figure 7). While the contours at 5 s reveal irregularities in the temperature distribution within the target, the final contours approximately follow the shape of the ice surface, suggesting an isothermal ice surface. This confirms that the system has entered the steady state at the end of the simulation.
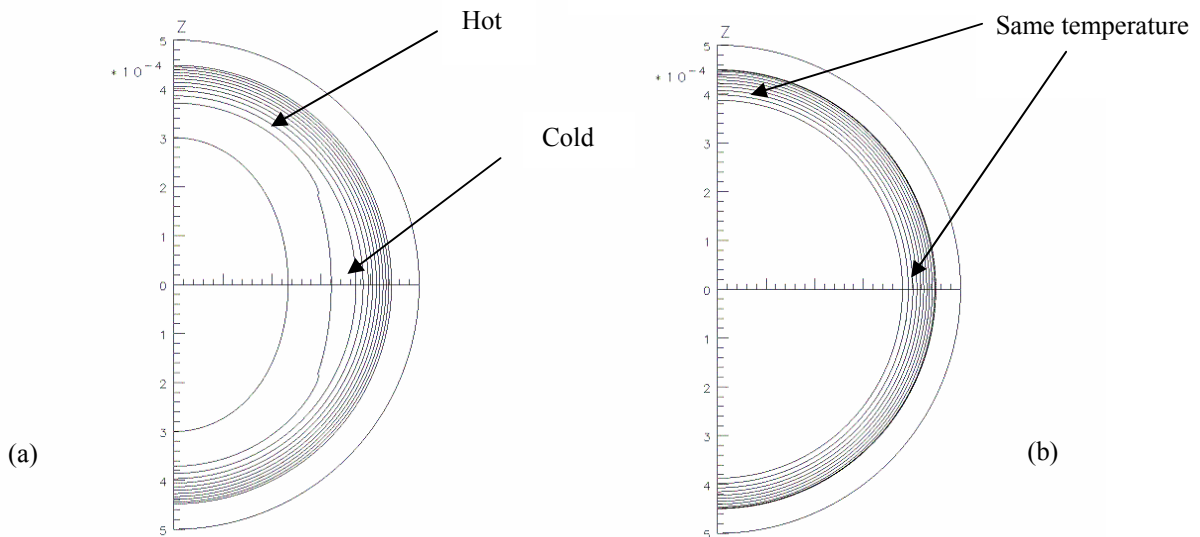

Figure 7: (a) Temperature contours in the target near the beginning of the layering process (t=5 s). The presence of the ring noticeably affects the contours near the equator. The distorted contour shows that the ice surface near the equator is colder than the surface near the poles. (b) Contours after the layering (t=1 h). The z axis is vertical and the outer radius is 500 μm. The outer radius of the target itself is 450 μm.

Figure 8 illustrates the temperature distribution as a function of radius at the

equator ($\theta = 90°$) and at the pole ($\theta = 0°$) in the vicinity of the ice layer, (a) after five

seconds and (b) after an hour. Near the beginning of the layering process, there is a small

but noticeable difference in temperature between the polar and equatorial regions. After

layering, the temperature at the D_2 ice/gas interface is uniform. Also, note the parabolic

temperature profile in the ice layer. The temperature gradient increases towards the outer

surface because the heat flux at each radius must equal the total IR heat deposited inside

that radius. Since the heat flux on either side of the outer ice surface is the same, the low

thermal conductivity of the helium gas causes a steep temperature gradient outside the

ice. There is also a small temperature gradient in the D_2 gas, because of the infrared

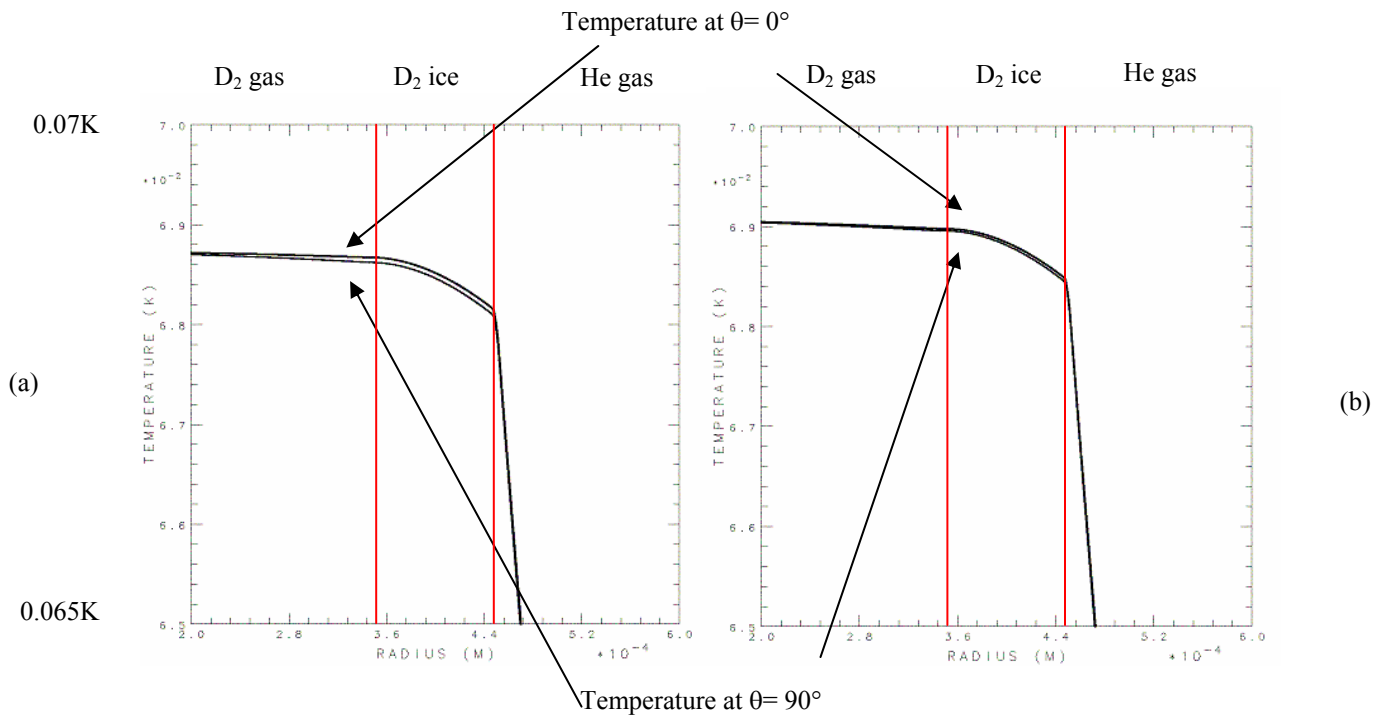heating of the gas. The temperature difference across the ice is about 500 µK, and there

Figure 8: (a) Temperature profile as a function of radius from 200 µm to 600 µm near the beginning of the layering process (t=5 s). (b) Temperature profile after layering (t=1 h). The temperatures on the scale represent the temperature above the reference temperature of 18.6 K. The vertical red lines indicate the ice layer (from 347 µm to 447 µm).

is about 0.1 K of difference between the outside of the target and the edge of the layering sphere. The figure indicates that the ice surface temperature approaches uniformity with respect to θ during the layering process.

Figure 9 plots the ice thickness against θ. The red line represents the initial thickness, which is uniform, and the blue line indicates the result after layering. The ice is slightly thicker (the interface radius is smaller) in the equatorial region (θ=90°).

Figure 9 shows that the maximum interface radius after layering is 347.6 μm, which occurs at the poles (θ=0°or θ=180°). The minimum radius, reached at the equator (θ=90°), is 346.3 μm. The largest deviation from the mean radius, which happens at the equator, is about 0.7 μm. As the deviation is within the design tolerance of 1 μm, we may conclude that the ring does not pose a significant threat to ice uniformity.
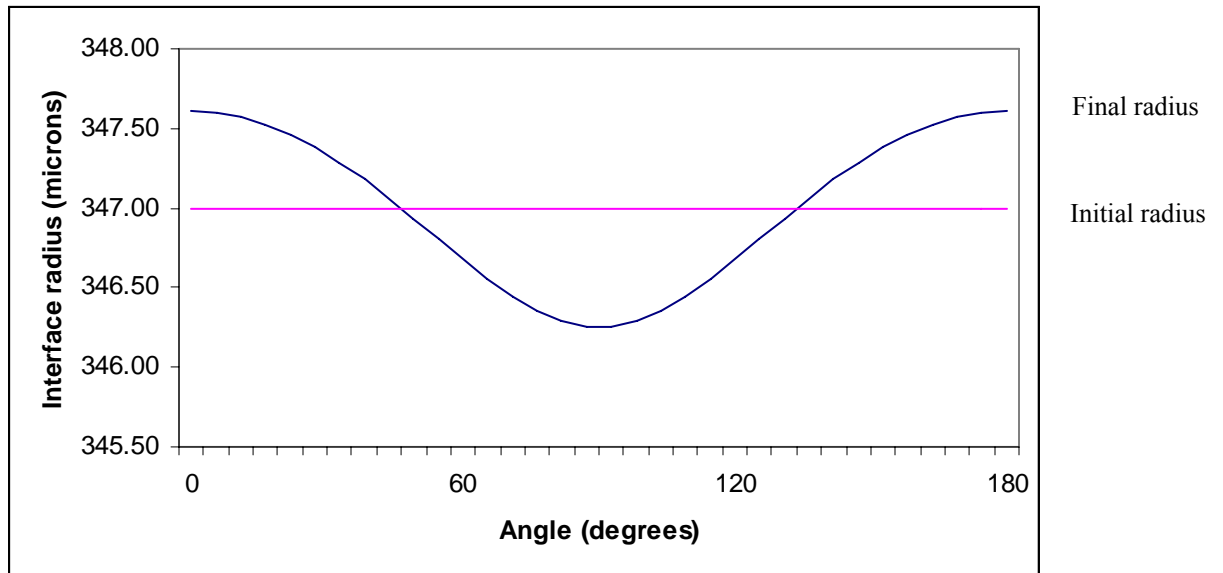

Figure 9: Ice-gas interface radius for different angles θ. The red and blue lines represent the initial and the final radii, respectively. The initial radius was set to be uniform as a function of θ. After layering, the ice becomes slightly thicker (the interface radius slightly smaller) near the equator (θ = 90°) and slightly thinner at the poles (θ = 0° and θ = 180°).

4. Conclusion

A new computer program has been developed to simulate the layering of a cryogenic target. A set of nonlinear partial differential equations was established to model the layering process. The equation set was decomposed into two parts, a linear partial differential equation set and a few linear and nonlinear functions. This significantly reduces computation complexity without noticeably sacrificing calculation accuracy. The interface cells are modeled as a linear mixture of gas and ice.

The program was applied to determine the ice shape after layering for "Saturn ring" targets. Two schemes were developed to reduce the number of time steps. First, the problem was cast into the framework of finding the steady state solution and the calculation was expedited by starting from an appropriate initial condition. Second, a variable time step size was implemented. A larger step size was adopted when the system is slowly varying to ensure computational efficiency, and a smaller time step is used when the system is rapidly changing to avoid large approximation errors.

The result showed that the nonuniformities caused by the plastic rings are small. The largest deviation from the mean radius is about 0.7 μm. This deviation is within the design tolerance of 1 μm, so its impact on fusion performance is acceptable.

5. Acknowledgements

I would especially like to thank Dr. Craxton for giving me the opportunity to participate in this wonderful program, as well as for the endless hours spent helping me with my project. I would also like to thank the fellow students in the LLE High School Summer Research Program for making this summer such a memorable experience.

References

[1] J. Nuckolls, et al., *Laser Compression of Matter to Super-High Densities: Thermonuclear (CTR) Applications,* **Nature** Vol. 239, p. 139 (1972).

[2] J. D. Lindl, *Development of the indirect-drive approach to inertial confinement fusion and the target physics basis for ignition and gain*, **Physics of Plasmas** Vol 2, p.3933 (1995).

[3] R. S. Craxton and D. W. Jacobs-Perkins, *The Saturn Target for Polar Direct Drive on the National Ignition Facility*, **Physics Review Letters** Vol 94, p. 095002 (2005).

[4] C. Stoeckl, et al., *First Results from Cryogenic Target Implosions on OMEGA.* **Physics of Plasmas** Vol. 9, p. 2195 (2002).

[5] D. N. Bittner, et al., *Forming Uniform HD Layers in Shells Using Infrared Radiation,* **Fusion Technology** Vol. 35, p. 244 (1999).

[6] E.L. Alfonso, *Modeling the Temperature and Ice-Thickness Profiles Within OMEGA Cryogenic Targets.* **LLE Review** Vol. 81, p.14 (2002).

 [7] D. Harding, private communication (2005).

Appendix. List of Physical Constants Used[6,7]

	K (W/mK)	C_v (J/(m^{3}K))	Q_{IR} (W/m^3)	L (J/molecule)
Solid D$_2$	0.38	5.802 x 10^5	4.6 x 10^4	9.80 x 10^{-22}
Plastic	0.05	1.95 x 10^5		
Helium	0.0227	0.969		
D$_2$ gas	0.009	2155	4.6	

T_{ref}	18.6 K
N_0	4.89 x 10^{22} molecules/(m^{2}s)
α	2.43 x 10^{22} molecules/(m^{2}sK)
β	7.84 x 10^{-4} m/s
γ	-2.11 x 10^{-5} m/(sK)